

# Plasma Acceleration in a Compact Helicon Source Using RF Antennae

Kyoichiro Toki,<sup>1</sup>

*Tokyo University of Agriculture and Technology, 2-24-16 Naka-cho, Koganei-city, Tokyo 184-8588 JAPAN*

Shunjiro Shinohara,<sup>2</sup>

*Kyushu University, 6-1 Kasuga-koen, Kasuga, Fukuoka 816-8580, JAPAN*

Takao Tanikawa,<sup>3</sup>

*Tokai University, 1117 Kitakaname, Hiratsuka, Kanagawa 259-1292, JAPAN*

Tohru Hada,<sup>4</sup>

*Kyushu University, 6-1 Kasuga-koen, Kasuga, Fukuoka 816-8580, JAPAN*

Ikkoh Funaki,<sup>5</sup>

*Japan Aerospace Exploration Agency, 3-1-1 Yoshinodai, Sagami-hara, Kanagawa 229-8510, JAPAN*

Kostiantyn P. Shamrai<sup>6</sup>

*Institute for Nuclear Research, National Academy of Sciences, 47 Prospect Nauki, Kiev 03680, UKRAINE*

Yoshikazu Tanaka,<sup>7</sup>

*Tokyo University of Agriculture and Technology, 2-24-16 Naka-cho, Koganei-city, Tokyo 184-8588 JAPAN*

and

Akihiro Yamaguchi<sup>8</sup>

*Tokyo University of Agriculture and Technology, 2-24-16 Naka-cho, Koganei-city, Tokyo 184-8588 JAPAN*

(Received: 31 August 2008 / Accepted: 6 December 2008)

The helicon wave excitation is one of the promising RF plasma production associated with a high density plasma ( $\sim 10^{13} \text{ cm}^{-3}$ ) that enables electromagnetic acceleration. We newly employed an acceleration coil or 2 pairs of copper plates around the 2.5 cm o. d. glass tube. These methods are called a repetitious coil current acceleration and a continuous “Lissajous” acceleration, respectively. In case of the repetitious coil acceleration, the maximum plasma velocity of 3.6 km/s was obtained with a 76% velocity increment with the absorbed plasma production + acceleration power of (400+180) W and the applied magnetic field strength of 1,450 gauss. As for the “Lissajous” acceleration, the plasma velocity was 2.2 km/s with the absorbed plasma production + acceleration power of (290+200) W.

Keywords: electrodeless, electromagnetic acceleration, helicon, plasma production, plasma acceleration

## Nomenclature

$B$	=	magnetic field
$u$	=	velocity
$e$	=	electronic charge
$E$	=	electric field
$I$	=	probe current
$J$	=	current
$m$	=	ion, neutral and electron mass
$t$	=	time
$\nu$	=	collision frequency
$\omega$	=	angular velocity

## Subscripts

0	=	initial
e	=	electron
ela	=	elastic
i	=	ion

inela	=	inelastic
para	=	pararell
perp	=	perpendicular
$x$	=	$x$ direction
$y$	=	$y$ direction
$z$	=	$z$ direction

## 1. Introduction

Recently electric propulsions have attracted wider attention with increasing opportunities in space applications because of their capability to save more propellant than the conventional chemical propulsions. For this reason, the electric propulsions are employed for long-term missions, such as interplanetary flight and satellite attitude control. This implies that the electric

*This work supported by Grant-in-Aid for Scientific Research (A), 17206084, Japan Society for the Promotion of Science*

*1. toki@cc.tuat.ac.jp, 2. shinohara@aes.kyushu-u.ac.jp, 3. tnth@keyaki.cc.u-tokai.ac.jp, 4. hada@esst.kyushu-u.ac.jp, 5. funaki@isas.jaxa.jp,*

*6. kshamrai@kinr.kiev.ua, 7. 50007643303@st.tuat.ac.jp, 8. 50004255119@st.tuat.ac.jp (The leading author, Prof. Toki was deceased on May 26, 2009.)*

propulsion is required very long lifetime in order to keep working for many years.

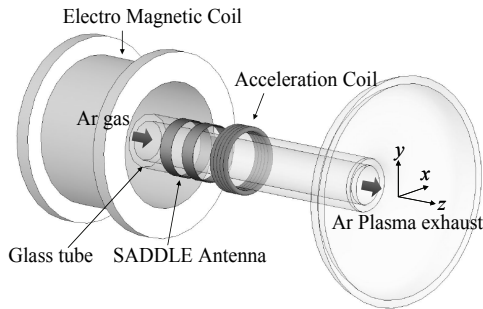
The electrodeless configuration is one of the long lived electric propulsion solutions free from electrode erosions [1-2], for example, VASIMR (Variable Specific Impulse Magnetoplasma Rocket). This plasma source based on the helicon plasma excitation which is one of the RF plasma production methods [3-4]. The VASIMR also employs a magnetic nozzle acceleration depending on the ICRH (Ion Cyclotron Resonance Heating) as the plasma energisation, hence VASIMR can avoid deterioration of the engine caused by electrode erosion [5]. However, the acceleration principle is based upon “plasma heating” and “passive nozzle expansion” categorized into an electrothermal regime. Here, we would like to propose an “electrodeless electromagnetic acceleration” in smaller thrusters than VASIMR.

This paper describes a new type small electrodeless electromagnetic thruster. A compact helicon plasma source was prepared to produce high density plasma ( $\sim 10^{13} \text{ cm}^{-3}$ ) that enables the electromagnetic acceleration. We already successfully established a helicon mode plasma in a 2.5 cm i.d. glass tube [6-8]. The plasma acceleration methods are divided into three categories. They are electrostatic or electromagnetic acceleration in addition to electrothermal acceleration such as VASIMR. Our plasma acceleration is based on electromagnetic principle [6], and employed two types of plasma methods using a coil or an RF antenna.

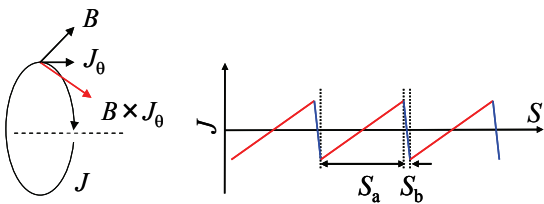
## 2. Principles of Electromagnetic Acceleration

### A. Repetitious Coil Current Acceleration of Plasma

The first approach is the coil current acceleration that induces a diamagnetic electron current in the azimuth



(a) Schematic of Coil acceleration device.



(b)  $J$  induced in plasma. (c) A saw-tooth current for the Coil.

Fig. 1. Principle of a repetitious coil current acceleration.

direction with its amplitude proportional to the time gradient of the applied magnetic field. The coil current induced has a saw-tooth current waveform. When the Lorentz force acts as an acceleration direction in a certain period, the plasma is compressed and directly accelerated toward downstream direction while the plasma is decelerated during the reversed change of the coil current. In order to prevent cancellation of acceleration with this deceleration phase, we took advantage of the difference of the skin time between the acceleration and the deceleration phases. The deceleration current decreases rapidly, while the acceleration current increases slowly. In this process, the deceleration force acts only the plasma periphery and the acceleration force acts the bulk plasma. The ideal wave form is shown in Fig.1.

### B. Continuous “Lissajous” Acceleration of Plasma

Secondly, we proposed 2 pairs of deflection plates around the glass tube to generate rotating electric field so as to induce electron current continuously in azimuth direction inside the cylindrical plasma. The ion current is scarcely induced because of its larger inertia. This is called as “Lissajous” acceleration but this approach requires important premises of the electric field penetration into high density plasma. The analysis of plasma acceleration is explained by using MHD equations including  $\mathbf{j} \times \mathbf{B}$  term and  $\mathbf{E}$  must include the collective plasma response.

$$m \frac{du_x}{dt} = eE_x - m\nu u_x + eu_y B_z \quad (1)$$

$$m \frac{du_y}{dt} = eE_y - m\nu u_y - eu_x B_z \quad (2)$$

Here,  $x, y, z$  are the coordinates depicted in Fig. 2 and  $\omega_0 = eB/m$ . The solution of these differential equations includes a general solution decaying exponentially by  $-\nu t$  and then only a special solution is valid and finally remained as expressed below.

$$u_x = \frac{eE_0}{m} \frac{1}{\sqrt{(\omega_0 - \omega)^2 + \nu^2}} \sin(\omega t + \phi) \quad (3)$$

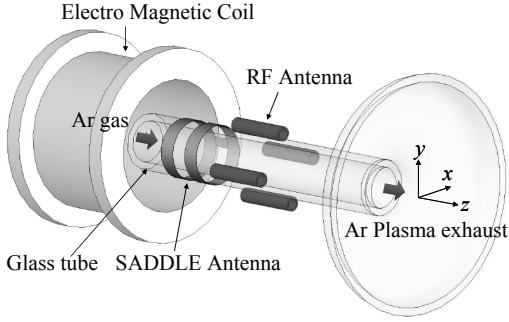
$$u_y = \frac{eE_0}{m} \frac{1}{\sqrt{(\omega_0 - \omega)^2 + \nu^2}} \cos(\omega t + \phi) \quad (4)$$

$$\tan \phi = \frac{\omega_0 - \omega}{\nu} \quad (5)$$

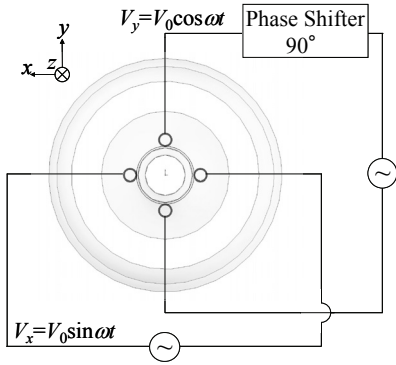
$$\nu = \nu_{ela} + \nu_{inela} \quad (6)$$

As far as the collision frequency  $\nu$  remains in a finite value, not the ions but the electrons due to the inertia difference, mainly contribute to rotational velocity and current around z-axis by rotating applied electric

fields of  $E_x$  and  $E_y$ . The collision frequency must involve elastic  $\nu_{ela}$ , inelastic  $\nu_{inela}$  collisions and charge exchange collisions  $\nu_{cex}$ , if necessary.



(a) Schematic of "Lissajous" acceleration device.



(b) Concept of Rotation Electric field.

Fig. 2. Principle of Continuous "Lissajous" Acceleration.

### 3. Experimental Procedures

#### A. Experimental Devices

Our compact helicon source consists of plasma production portion, plasma acceleration portion and a vacuum system. A 2.5 cm i.d. with totally about 30 cm long pyrex glass tube connected to a vacuum chamber (Fig. 3). Ar gas is supplied from a metallic end plate with a gas port to the glass tube. The RF power for plasma production and acceleration are applied during the Ar gas flow along the glass tube toward the vacuum chamber. A double saddle type (Boswell type) antenna is used for plasma production, and a 47 turn acceleration coil or a pair of acceleration antennae downstream are used for acceleration. The vacuum chamber is evacuated down to 0.1 Pa (1 mTorr) or lower, and the Ar gas is fed by a mass flow controller Brooks 5850E at a predetermined mass flow rate, 0.5 mg/s corresponding to the background pressures of 0.1 Pa (1 mTorr). A 489 turn coil magnet produces 38 gauss/A up to 1,450 gauss maximum in the midst of coil bobbin. A signal generator of HP-8657A and a 500 Wmax amplifier of Thamway T145-5768A with a matching box T020-5558A at the frequency 27.12 MHz for plasma production, and T145-5536 with

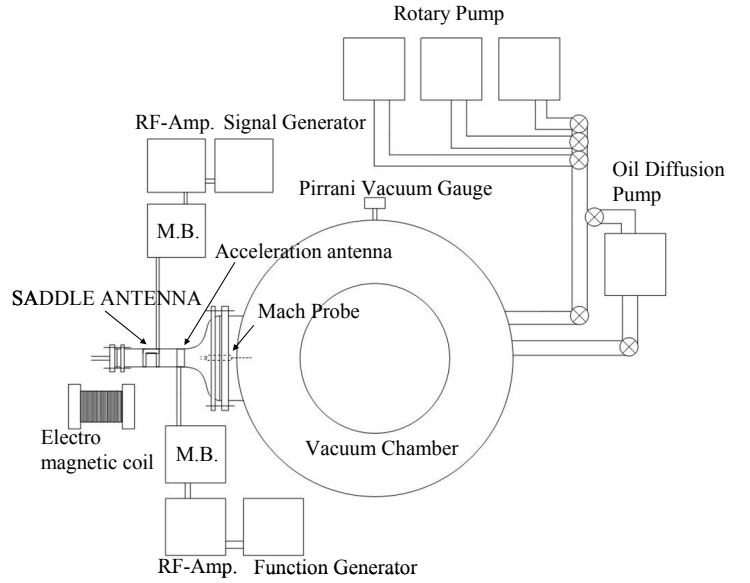


Fig. 3. Experimental devices.

T020-5536A for 300 W acceleration amplifier with frequency range of 1-16 MHz were used for RF power source. In case of the continuous Lissajous acceleration, two RF signals with external phasing each other are amplified and input to the antennae via separate matching boxes.

#### B. Probe for Measuring Plasma Velocity

We used a Mach probe shown in Fig. 4. [7] The Mach probe comprises two tips facing parallel and perpendicular to the plasma flow. Our Mach probe was made from 1.5 mm diam. copper rods with 45 degrees tapered surfaces, the one parallel and the other perpendicular to the flow. These rods are covered by 2 mm in diam. ceramic tubes. Here, ion acoustic Mach number  $M_i$  is defined by ratio of plasma velocity to the ion acoustic velocity  $C_s$ .

$$M_i = \frac{U}{C_s} = \frac{U}{\sqrt{\frac{\gamma_e T_e + \gamma_i T_i}{m_i}}} \quad (7)$$

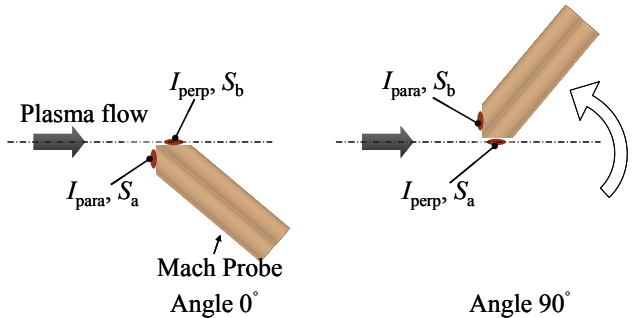


Fig. 4 Mach probe rotates around the centerline of the plasma.

The ion acoustic Mach number  $M_i$  is expressed as the

ratio of ion saturation currents collected by two probe tips.

$$\frac{I_{para}}{I_{perp}} = \frac{M_i}{\kappa} \quad (8)$$

$$\frac{I_{para}}{I_{perp}} = \exp(aM_i^{1/a}), \quad a = -\ln \kappa \quad (9)$$

Where,  $\kappa$  is dependent on the ratio of  $T_i/T_e$ . In a supersonic flow ( $M_i > 1$ ), Eq.(8) is used. But, in a subsonic flow ( $M_i < 1$ ), Eq.(9) is used.

To minimize the probe interactions with the plasma ignition, the ceramic insulator as thin as 2 mm o.d. diam. tube was used. The probe voltage was applied by a battery from -60 to +60 V. The probe current was measured by a simple resistor. Both the probe voltage and current traces are recorded by an Omniace RA1200 digital recorder and then analyzed by a personal computer. The electron temperature was evaluated from the gradient of probe curve near the floating potential and the plasma density was calculated from the ion saturation current.

To improve measurement accuracy, we developed a probe assembly driver rotatable around the edge of Mach probe and making 2 positions at the angle of  $0^\circ$  or  $90^\circ$  degrees. It enables to estimate the ratio of probe tips area with sheath layer. Thus, we can obtain the tip area ratio by using this assembly. If the ratio of ion saturation currents at the angle of  $0^\circ$  is equal to that of  $90^\circ$ , their relationship is expressed below.

$$\frac{I_{para}}{I_{perp}} \cdot \frac{S_b}{S_a} = I_0 \quad \frac{I_{para}}{I_{perp}} \cdot \frac{S_a}{S_b} = I_{90} \quad (10)$$

Here,  $S_a$  and  $S_b$  are the area of probe tip a and b, respectively. Consequently, the ratio of probe tips area is expressed as the following.

$$\frac{S_a}{S_b} = \sqrt{\frac{I_{90}}{I_0}} \quad (11)$$

By applying Eq.(11), we obtain the ratio of  $I_{para}$  and  $I_{perp}$  with high precision.

#### 4. Experimental Results

Firstly, the axial and radial magnetic field intensity were measured by gauss meter. The axial distance of 0 mm is the edge of double saddle type antenna set-up point and axial distance of 20 mm is in the midst of coil bobbin. The magnetic field intensity at the acceleration point (90 mm) was 800 gauss. The maximum of radial magnetic field intensity was 330 gauss.

##### A. Repetitious Coil Current Acceleration Results

The measurement for various acceleration powers up to 180 W were conducted. The tips of the Mach probe

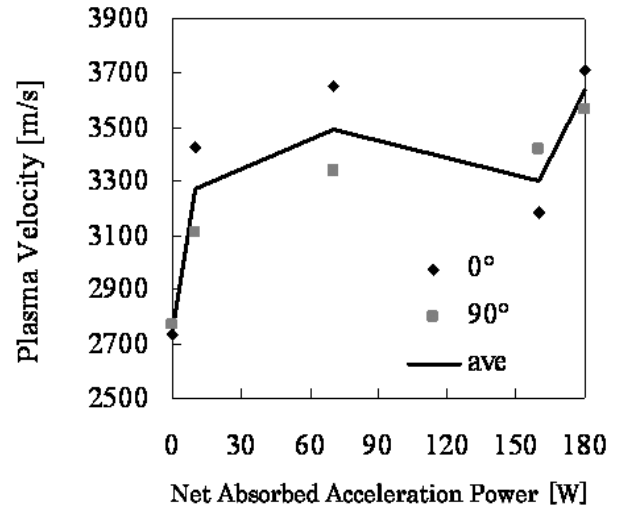


Fig. 5. Plasma velocity measurement of a repetitious coil current acceleration at each absorbed RF power ( $0^\circ$  and  $90^\circ$  are the angles in Fig. 4).

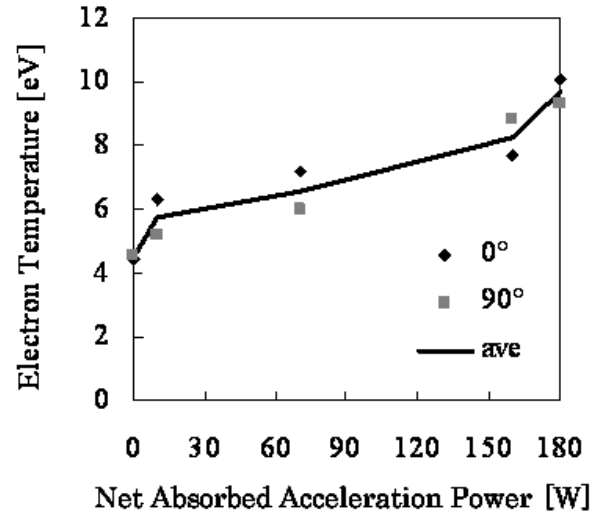


Fig. 6. Electron temperature of a repetitious coil current acceleration at each absorbed RF power ( $0^\circ$  and  $90^\circ$  are the angles in Fig. 4).

were placed along the centerline of glass tube about 6.5 cm downstream position from the edge of the acceleration coil. The 47 turn coil for plasma acceleration was wound around the 2.5 cm glass tube. The repetitious coil current acceleration is done under the chamber pressure of 0.10 Pa, Ar gas flow rate of 0.4 mg/s, the forward plasma production power of 400 W at a frequency of 27.12 MHz, a plasma acceleration frequency for the coil of 6 MHz, and the applied magnetic field strength of 1,450 gauss. The applied saw-tooth waveform exhibited the rise-time of 170 ns and the fall-time of 17 ns, actually not so sharp as shown in Fig. 1 (c).

The plasma velocity, electron temperature and plasma density are shown in Fig. 5- Fig. 7. Here, “net absorbed acceleration power” means the forward power minus reflection power. The diamond and square plots are the data for the probe angle of  $0^\circ$  and  $90^\circ$  degrees,

respectively. The solid line implies the averaged data at  $0^\circ$  and  $90^\circ$ . Figure 5 shows plasma velocity increases, as

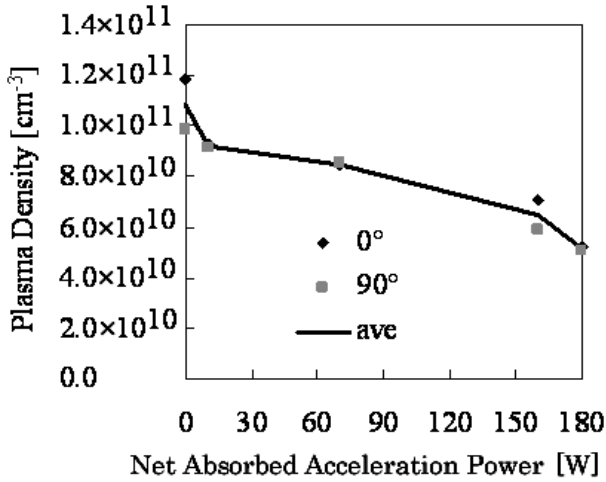


Fig. 7. Plasma density of a repetitious coil current acceleration at each absorbed RF power ( $0^\circ$  and  $90^\circ$  are the angles in Fig. 4).

the applied acceleration power increases. The velocity was increased by 76 % compared with the value before acceleration at the max power of 180 W. Similarly, the more the applied acceleration power increases, the more the electron temperature increases. At the maximum power of 180 W, it indicates about 2.2 times increase compared with before acceleration. This implies that the plasma velocity increase was brought about by thermal acceleration process. On the other hand, the plasma density is decreased as the plasma is accelerated. Thus, the product of density  $\times$  electron temperature seems to be constant with RF power. When we adopted a repetitious coil current acceleration method, the RF power was absorbed into electrons to raise the electron temperature and this results in the electrothermal acceleration. Our final goal is to have plasma electromagnetically accelerated. At present, we have found that one of the reasons of insufficient electromagnetic acceleration is due to the incomplete formation of the saw-tooth waveform. The required steep gradient of the deceleration period is moderated by the filter of the matching box. The coil current through the matching box, the saw-tooth waveform tends to change into a sinusoidal waveform. We should solve this problem in the next step.

### B. Continuous “Lissajous” Acceleration Results

Figures 8-10 exhibit the results of measured plasma velocity, electron temperature and plasma density for “Lissajous” acceleration. The tips of the Mach probe are placed 6.5 cm downstream location from the edge of the antennae and rotated at the position. We tried a

continuous “Lissajous” acceleration under the conditions of the chamber pressure of 0.13 Pa, Ar gas flow rate of

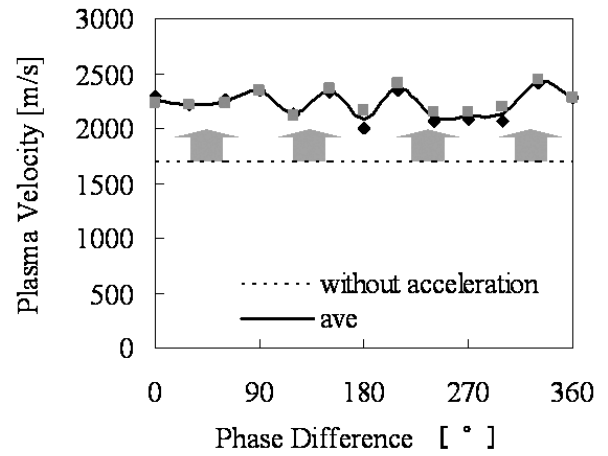


Fig. 8 Plasma velocity at each phase difference in “Lissajou” acceleration ( $0^\circ$  and  $90^\circ$  are the angles in Fig. 4).

0.5 mg/s, the absorbed plasma production power of 290 W at frequency of 13.56 MHz, the absorbed plasma

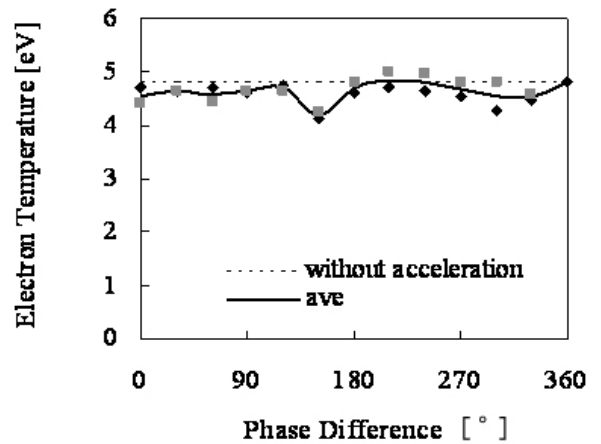


Fig. 9 Electron temperature at each phase difference in “Lissajous” acceleration ( $0^\circ$  and  $90^\circ$  are the angles in Fig. 4).

acceleration power of 200 W at frequency of 15 MHz and the applied magnetic field strength of 1,450 gauss.

The diamond and square plots are the data which represent the probe angle of  $0^\circ$  and  $90^\circ$  degrees, respectively. The solid line in the figures is average of measuring data at  $0^\circ$  and  $90^\circ$  probe positions and dotted line denotes the case applied only plasma production power. In Fig. 8, it was recognized that the plasma velocity was increased by 50% compared to the before acceleration and resulted in 2.2 km/s. This is not satisfactory result because our goal in this power level is 14 km/s corresponding to 50% thrust efficiency. This result implies that only a little amount of the acceleration

power was absorbed by plasma and the rest of the power was dissipated as circuit loss or vacuum loading.

The electron temperature revealed small decrease at all phase differences. This indicated that the power for acceleration was not absorbed by electrons. On the contrary, the plasma density showed slight increase at all phase differences. This result implies that the plasma was created by applying RF power of acceleration, or other factors like plasma space potential have some effects on this measurement. The principle of continuous “Lissajous” acceleration is based on electrons rotational drift motion. The RF electric field penetrating radially into plasma was not measured but predicted by Shamrai

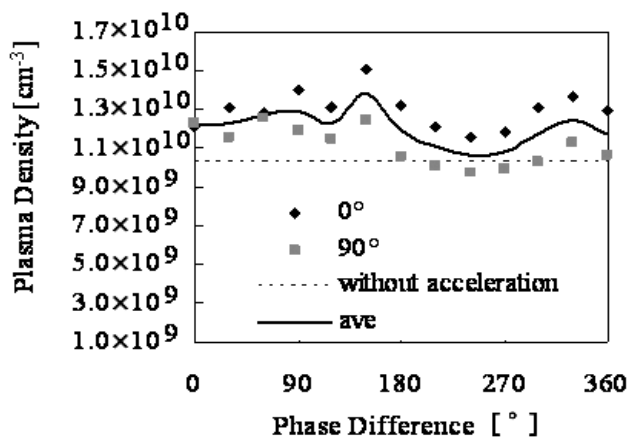


Fig. 10 Plasma density at each phase difference ( $0^\circ$  and  $90^\circ$  are the angles in Fig. 4).

about 10 V/cm at the plasma center and this value increases toward the plasma periphery [8]. The acceleration profile in radial direction is similar to this electric field distribution. However, as shown in Fig. 8, the plasma velocity did not reveal remarkable acceleration / deceleration corresponding to the sign change of electron motion with the phase difference. The electromagnetic acceleration may not fully take place but the electrothermal acceleration is dominant because the

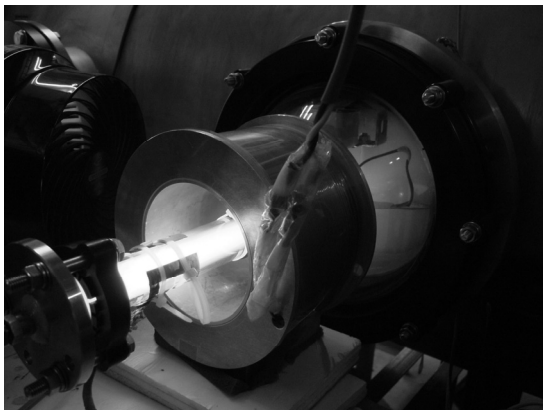


Fig. 11. Experiment of a repetitious coil current acceleration.

collision between electrons and neutrals under this pressure is nearly equal to the acceleration frequency. To avoid this problem, we should maintain the acceleration region at higher vacuum condition than ever. This situation would be realized to lower the Ar gas flow rate, to place whole the device inside the vacuum chamber, or to increase the acceleration frequency of the amplifier. We need to ascertain the best shape of RF antenna for the plasma electromagnetic acceleration attempting various RF matching conditions for higher absorption efficiency.

Figure 11 is an experiment of a repetitious coil current acceleration. In the interior of the magnetic coil of the bottom picture, the plasma emits blue light. This shows a so-called “blue mode” of helicon wave excited plasma.

## 5. Conclusion

For the repetitious coil current acceleration method, the maximum plasma velocity was 3.6 km/s. It was 76 % velocity increment compared with the value before acceleration under the chamber pressure of 0.10 Pa, Ar gas flow rate of 0.4 mg/s, the absorbed plasma production and acceleration power of (400+180) W, the coil of 47 turns and the applied magnetic field strength of 1,450 gauss. However, the electron temperature was raised up to about 2.2 times higher than the value before acceleration. This implies that the increment of plasma velocity is done by thermal process.

For the continuous “Lissajous” acceleration method, the plasma velocity was 2.2 km/s under the chamber pressure of 0.13 Pa, Ar gas flow rate of 0.5 mg/s, the absorbed plasma production and acceleration power of (290+200) W, the coil of 47 turns and the applied magnetic field strength of 1,450 gauss.

## 6. References

- [1] K. P. Shamrai, et al., J. Physics IV, France 7, C4, pp. 365-381 (1997).
- [2] K. Toki, et al., IEPC 03-0168, Proc. of the 28th International Electric Propulsion Conference, Toulouse (2003).
- [3] S. Shinohara, J. of Plasma and Fusion Research, 78, 1, pp. 5-18 (2002).
- [4] C. Charles, R. Boswell, et al., AIAA-2006-4838, 42nd AIAA/ASME/SAE/ASEE Joint Propulsion Conference & Exhibit, Sacramento (2006).
- [5] J. P. Squire, F. R. Chang Diaz, et al., AIAA 2000-3752, 36th AIAA/ASME/SAE/ASEE Joint Propulsion Conference, Huntsville (2000).
- [6] K. Toki, S. Shinohara, T. Tanikawa and K. P. Shamrai, ELSEVIER, Thin Solid Films, 506-507, pp. 597-600 (2005).
- [7] A. Ando, et al., J. of Plasma and Fusion Res., 81, 6, pp. 451-457 (2005).
- [8] K. Toki, et al., AIAA 2004-3935, 40th AIAA/ASME /SAE /ASEE Joint Propulsion Conference, Huntsville (2004).